Reliable Adaptive Modulation Aided by Observations of Another Fading Channel

Tung-Sheng Yang, Alexandra Duel-Hallen, and Hans Hallen

Abstract— **Adaptive transmission techniques, such as adaptive modulation and coding, adaptive power control, adaptive transmitter antenna diversity, etc., generally require precise channel estimation and feedback of channel state information (CSI). For fast vehicle speeds, reliable adaptive transmission also requires long range prediction (LRP) of future CSI since the channel conditions are rapidly time-variant. In this paper, we propose to use past channel observations of one carrier to predict future CSI and perform adaptive modulation without feedback for another correlated carrier. We derive the minimum mean-square-error (MMSE) long range channel prediction that utilizes the time and frequency domain correlation function of the Rayleigh fading channel. An adaptive MMSE prediction method is also proposed. Statistical model of the prediction error that depends on the frequency and time correlation is developed and is used in the design of reliable adaptive modulation methods. We use a standard stationary fading channel model (Jakes model) and a novel physical channel model to test our algorithm. Significant gains relative to non-adaptive techniques are demonstrated for sufficiently correlated channels and realistic prediction range.**

Index Terms—**Adaptive modulation, multipath fading, fading channel prediction, physical channel modeling, multiple carriers.**

I. Introduction

High speed wireless communications require robust channel estimation and adaptive transmission to satisfy the tremendous growth in demand for capacity. The idea of adaptive transmission [1–4] is to vary the transmission parameters according to the instantaneous fading channel power without sacrificing the bit-error rate (BER). For example, adaptive modulation methods can provide higher bit rates relative to conventional signaling by transmitting at high rate under favorable channel conditions, and reducing the throughput as the channel degrades. These adaptive modulation techniques depend on accurate channel state information (CSI) that can be acquired from different sources. If the communication between the two stations is bi-direction and the channel can be considered reciprocal, as, for example, in time division duplex (TDD) systems, then each station can estimate the channel quality on the basis of the received symbols and adapt the parameters to this estimation. This is called open-loop adaptation [5]. If the channel is not reciprocal, the receiver has to estimate channel quality from feedback resulting in closed-loop adaptation. The feedback load consumes power and bandwidth, and the fed back CSI needs to be quantized resulting in degraded performance. Note that for many adaptive transmission applications (e.g., selective transmitter diversity or adaptive modulation [9]), it is not necessary to feed back the actual fading coefficient. It is sufficient to send to the transmitter just the antenna selection or modulation index bits derived from the estimates of predicted values at the receiver. The feedback delay, overhead, channel estimation and CSI quantization errors, and processing delay degrade the performance of adaptive modulation, especially in rapidly time variant fading. Even in open-loop channels, current CSI is not sufficient since future channel conditions need to be known to adapt transmission parameters. To realize the potential of adaptive transmission methods, the channel variations have to be reliably predicted at least several milliseconds ahead.

Recently, a novel adaptive long-range prediction (LRP) method was proposed in [6–9]. This algorithm employs an autoregressive (AR) model to characterize the fading channel and computes the minimum mean-square-error (MMSE) estimate of a future fading coefficient based on a number of past observations. The advantage of this algorithm relative to conventional methods is due to its low sampling rate (on the order of twice the maximum Doppler shift and much lower than the data rate), which results in longer memory span and further prediction into the future for a fixed filter length. The low sampling rate also results in reduced feedback rate.

In this paper and [14,18], we extend the long-range prediction algorithm into frequency domain. In particular, we concentrate on the scenario where we observe a received uplink signal at the carrier frequency f^1 and attempt to predict the downlink signal at the carrier frequency f^2 without feedback from the mobile. Alternatively, a signal at frequency f^1 can be fed back and a signal at adjacent frequency f^2 is predicted without feedback. To accomplish this prediction, the predicted samples must be sufficiently correlated with the observations in both time and frequency. This technique can be applied in correlated uplink and downlink channels as in Frequency Division Duplex (FDD) systems, in orthogonal

Manuscript received Auguest 12, 2002; revised September 10, 2003. This paper was supported by NSF grants CCR-9815002 and CCR-0312294 and ARO grant DAAD 19-01-1-0638. This paper was presented in part at the IEEE WCNC'02, Orlando, March 17-21, 2002, and at the IEEE SPAWC'03, Rome, June 15-18, 2003.

T.S. Yang and A. Duel-Hallen are with the Department of Electrical and Computer Engineering, North Carolina State University, NC 27606 USA (e-mail: tsyang@unity.ncsu.edu; sasha@eos.ncsu.edu)

H. Hallen is with the Department of Physics, North Carolina State University, NC 27606 USA (e-mail: Hans_Hallen@ncsu.edu)

frequency division multiplexing (OFDM) systems (where narrow correlated sub-channels are employed) or other wideband systems to reduce feedback and overhead requirements.

The prediction accuracy of the aforementioned algorithm is determined by the rate of change of amplitude, frequency and phase of each path [6,9,12,17]. However, the standard Jakes channel model [10] or a stationary random process description does not capture the variation of these parameters. To validate the LRP algorithm, a novel physical channel modeling based on the method of images and augmented with diffraction is proposed in [9,12,17]. This physical model can generate non-stationary datasets to test both the LRP and its application in adaptive transmission scheme. It is demonstrated in [9,12,17] that this physical model generates datasets that closely resemble measured data, and results of the LRP for the physical model and measured data are similar, and differ significantly from those produced for the Jakes model. Thus, we have demonstrated that the proposed physical model is realistic. In addition, this model's insights allow classification of scenarios into typical and challenging cases for testing the algorithm. These scenarios are more difficult to identify with the measured data. In particular, in this paper, we use the physical model to examine the dependency of the correlation between two different carrier frequencies on the variation of the root mean square (*rms*) delay spread and to investigate the limits on the adaptation rate. Thus, the physical model allows us to test robustness and to determine practical constraints of the proposed adaptive transmission methods.

The remainder of this paper is organized as follows. In section II, we present the system model and describe the theoretical MMSE long-range prediction, a robust prediction method and the statistical model of the prediction error. In section III, the adaptive modulation scheme aided by the long-range prediction is discussed. Finally, section IV presents computer simulation results to demonstrate the prediction range in frequency domain. In this section, we extend the physical model to accommodate multiple carrier frequencies and use it to test the proposed channel prediction algorithm. We use this model to examine sensitivity of adaptive modulation performance to the variation of *rms* delay spread and identify typical and challenging situations encountered in practice.

II. Channel Statistics and System Model

A. Statistics of Mobile Radio Channel

The statistics of fading signals received at correlated carriers are discussed in [10]. The equivalent lowpass complex fading coefficients at two frequencies f^1 and f^2 can be expressed as:

$$c(f^i,t)=\sum_{n=1}^{N} A_n \exp\{j(2\pi f_n t+\phi_{in}\} \qquad i=1,2 \tag{1}$$

where for the n^{th} path, A_n is the (real) amplitude and f_n is the Doppler shift. The phase difference of the n^{th} path $\phi_{1n}-\phi_{2n}=2\pi\Delta f T_n$ where $\Delta f=f^2-f^1$ is the frequency separation, and T_n is the excess propagation delay. For large N, $c(f^i,t)$ is distributed approximately as a zero mean complex Gaussian random variable. (We assume $E[|c(f^i, t)|^2] = 1$.) Hence the amplitudes $\alpha(f^1,t)=|c(f^1,t)|$ and $\alpha(f^2,t)=|c(f^2,t)|$ are both Rayleigh distributed. Assume angular distribution of the incident power is uniform between $[0,2\pi]$, horizontal directivity pattern of the receiving antenna is 1, and the propagation delay T_n is exponentially distributed [10] with the probability density function (pdf):

$$p(T)=\frac{1}{\sigma}exp\{-\frac{T}{\sigma}\} \tag{2}$$

where σ is a measure (*rms* delay spread [11]) of the time delay spread. The cross-correlation of the two fading signals with the time difference $\tau=|t_1-t_2|$, maximum Doppler shift f_{dm} and the frequency separation $\Delta f=f^2-f^1$ can be derived as [15]:

$$R(\tau,\Delta f)=E[c(f^1,t)\,c^*(f^2,t+\tau)]=R_t(\tau)\,R_f(\Delta f) \tag{3}$$

where $R_t(\tau)=J_0(2\pi f_{dm}\tau)$ is the zero order Bessel function and $R_f(\Delta f)=\frac{1}{1+(2\pi\Delta f\sigma)^2}+j\frac{2\pi\Delta f\sigma}{1+(2\pi\Delta f\sigma)^2}$. Define $\Delta f\sigma$ as the normalized frequency separation. The cross-correlation (3) vs. $\Delta f\sigma$ for $\tau=0$ is plotted in Fig. 1. We also plotted the numerical cross-correlation of generated fading signals for comparison. To generate the signals, $c(f^1,t)$ was created first using the Jakes model [10]. In this paper, we employ the 9 oscillators Jakes model with the maximum Doppler shift $f_{dm}=100$Hz. Then $c(f^2,t)$ was generated from $c(f^1,t)$ using the same parameters except phase shifts as in (1). Multiple experiments were performed using independent realization of propagation delay T_n according to (2) and the ensemble average of cross-correlation was computed. Using this fading model and the non-stationary physical model employed in Section IV, we characterize the capability of the proposed method to enable adaptive modulation.

B. System Model and MMSE Long Range Prediction

The discrete-time system model is illustrated in Fig. 2. The frequency of observed CSI is f^1 and the frequency of transmitted signal is f^2. Let $c(f^n,i)$, $n=1,2$, be samples of the fading signal $c(f^n,t)$ at the sampling interval T_s. Assume stationary and ergodic time-varying complex channel gain sequence $\alpha(f^n,i)=|c(f^n,i)|$ with distribution $p_\alpha(x)$. The linear MMSE one-step prediction of the future channel sample $c(f^2,n)$ at frequency f^2 based on p previously observed samples $c(f^1,n-j)$ at frequency f^1 is given by:

$$\hat{c}(f^2,n)=\sum_{j=1}^{p} d_j c(f^1,n-j) \tag{4}$$

The optimal coefficients d_j are determined as:

$$\underline{d}=\underline{R}^{-1}\underline{r} \tag{5}$$

where $\underline{d}=(d_1 \cdots d_p)^T$. R is the autocorrelation matrix (p×p) with coefficients $R_{ij}=E[c^*(f^1,n-i)\,c(f^1,n-j)]$ and $\underline{r}$ is the autocorrelation vector (p×1) with coefficients $r_j = E[c^*(f^1,n-j)c(f^2,n)]$. The resulting MMSE is given by:

$$E[|e(n)|^2]=E[|c(f^2,n)-\hat{c}(f^2,n)|^2]=1-\sum_{j=1}^{p} d_j^* r_j \qquad (6)$$

In practice, the samples $c(f^1,n)$ are observed in the presence of additive white Gaussian noise (AWGN) z(i) with power spectrum density (PSD) N_0. Equations (4–6) can be easily modified to include noisy observations [7]. As p increases, the MMSE saturation level is approached. With the knowledge of the cross-correlation function (3), we can derive the closed form expression of MMSE for p = ∞ and one-step prediction. Let r(k) be the autocorrelation of the noisy fading channel samples $r(k) = E[(c(f^1,n-k) + z(n-k))\,(c(f^1,n) + z(n))^*] = R_n(k) + \delta(k)N_0$, where $R_n(k) = E\,[c(f^1,n-k)\,c^*(f^1,n)] = R_t(kT_s)$ is the discrete time autocorrelation function of the fading channel. Since r(k) is a correlation sequence, it can be represented as $r(k) = \sum_{j=-\infty}^{0} r^-(j)\, r^+(k-j)$ for all k, where $r^-(k)$ and $r^+(k)$ are the sequences that satisfy $r^-(k) = 0$ when k>0 and $r^+(k) = 0$ when k<0. From [15,16], d(z), the Z–transform of the filter d(n), can be derived as $d(z) = R_f(\Delta f)\,[z - \frac{1}{(r_z{}^+(z^*))^*\, r^+(0)]^*z]}$, where $r_z{}^+(\bullet)$ is the Z–transform of $r^+(k)$. Once the filter coefficients are known, we can calculate the MMSE in (6) as $MMSE = R_n(0) - b_0$, where b_0 is the power of predicted signal $\hat{c}(f^2,n)$ and can be derived as $b_0 = |R_f(\Delta f)|^2\,[r_n(0) - r_n^+(0)^2]$. Hence, the MMSE can be expressed as [15,16]:

$$MMSE=R_n(0)-|R_f(\Delta f)|^2[R_n(0)-r^+(0)^2+N_0] \qquad (7)$$

where $r^+(0)^2 = exp\{\frac{1}{2\pi}\int_{-\pi}^{\pi} \ln[R_w(w)+N_0]dw\}$, and $R_w(w) = \sum_{n=-\infty}^{\infty} R_n(n)exp\{-jwn\}$ is the folded power spectrum of the channel. In Fig. 3, the theoretical MMSE of one-step prediction (7) is plotted vs. normalized frequency separation $\Delta f\sigma$ for different values of the signal-to-noise ratio (SNR). The sampling rate $f_s = 5f_{dm}$ is chosen since it results in near optimal performance for LRP [7]. The prediction range is $0.2/f_{dm}$ seconds. We also compare the MMSE of the system with filter order p = 100 (see (4)). We found that for p =100, the MMSE approaches the optimal case (p = ∞) for $f_s = 5f_{dm}$. Throughout the paper, we employ p = 100 and the sampling rate of 500Hz assuming the maximum Doppler shift of 100Hz. The observation interval of 100 samples is used to estimate the autocorrelation function in the algorithm above and to achieve convergence in the adaptive method described below. The SNR in the observations is chosen as 80dB. In practice, noise-reduction techniques can be employed to reduce the noise present in the observations [7,9].

From the linear prediction algorithm (4), the predicted fading signal $\hat{c}(f^2,n)$ is a zero-mean complex Gaussian random variable. Later in the paper, we employ other Gaussian estimates. Suppose $\alpha=\alpha(f^2,t)$ is the actual fading amplitude, and $\hat{\alpha}$ is the amplitude of a zero mean complex Gaussian estimate correlated with $c(f^2,t)$. Thus, the pdf of $\hat{\alpha}$ is

$$p(\hat{\alpha})=(2\hat{\alpha}/\hat{\Omega})\,exp(-\hat{\alpha}^2/\hat{\Omega}) \qquad (8)$$

and the conditional pdf of α given $\hat{\alpha}$ is Rician given by[4,8]:

$$p(\alpha\,|\hat{\alpha}) = p(\alpha,\hat{\alpha}) / p(\hat{\alpha}) = \frac{2\alpha}{(1-\rho)\Omega}\, I_0\left(\frac{2\sqrt{\rho}\alpha\hat{\alpha}}{(1-\rho)\sqrt{\Omega\hat{\Omega}}}\right) exp\left(-\frac{1}{1-\rho}\left(\frac{\alpha^2}{\Omega}+\frac{\rho\hat{\alpha}^2}{\hat{\Omega}}\right)\right). \qquad (9)$$

where the correlation coefficient $\rho = \frac{Cov(\alpha^2,\hat{\alpha}^2)}{\sqrt{Var(\alpha^2)Var(\hat{\alpha}^2)}}$, $0 \le \rho \le 1$, $\Omega=E\{\alpha^2\} = 1$, $\hat{\Omega}=E\{\hat{\alpha}^2\}$, and I_0 is the 0^{th} order modified Bessel function. This conditional distribution will be used in the selection of modulation parameters in section III.

C. *Robust Long Range Prediction*

If the channel statistics, such as the time and frequency domain correlation, are known, the optimum MMSE channel prediction can be employed as in (4–5). However, as the Doppler shifts in (1) vary, the model coefficients need to be updated continuously based on the observations. Since we are not able to observe the fading coefficients at frequency f^2, we modify our approach as follows. First, we predict future channel coefficient $c(f^1,n)$ and then use the frequency correlation function to select the transmitter parameters at f^2. The predicted CSI at f^1 are given by:

$$\hat{c}(f^1,n)=\sum_{j=1}^{p} g_j^*(n)c(f^1,n-j) \qquad (10)$$

The coefficients $g_j(n)$ are determined using the Least Mean Square (LMS) adaptive tracking method:

$$g_j(n+1)=g_j(n)+\mu\varepsilon_n^*\hat{c}(f^1,n-j) \qquad (11)$$

where μ is the step size and $\varepsilon_n=c(f^1,n)-\hat{c}(f^1,n)$. This adaptive tracking can be performed since the observations at frequency f^1 are available at the transmitter [7,9]. The recursive least-squares (RLS) algorithm can also be used to improve accuracy and reduce the observation interval [12,17]. The coefficients $\hat{c}(f^1,n)$ are interpolated to obtain predictions at the symbol rate at frequency f^1 [6].

Once $\hat{c}(f^1,n)$ is found, the adaptive modulation parameters for transmitting at f^2 at time n are selected. (Note that $\hat{c}(f^2,n)$ is not predicted directly). As explained in section III, this procedure depends on the pdf of the $\alpha(f^2,n)$ given $\hat{\alpha}(f^1,n)$, If

we assume perfect CSI at frequency f^1 for sample n, this conditional pdf is determined by (9) with $\Omega = \hat{\Omega} = 1$ and

$$\rho = 1/(1+(2\pi\Delta f\sigma)^2) \tag{12}$$

In practice, this pdf is computed as in (9) using empirical estimates of $\hat{\Omega}$ and ρ and depends on the accuracy of prediction in (10). It can be shown that when the estimates $\hat{c}(f^1,n)$ are scaled so that $\hat{\Omega}=1$, the performance of adaptive modulation is not affected. Hence throughout the paper, $\hat{\Omega}$ is normalized to 1 for simplicity, and the performance depends only on the correlation coefficient ρ. The adaptation of ρ to the variation of the *rms* delay spread is discussed in section IV.

III. Adaptive Transmission Aided by Long Range Prediction

In this paper, we employ variable rate and variable power square multilevel quadrature amplitude modulation (M–QAM) signal constellations due to their inherent spectral efficiency and ease of implementation [1,13]. First, consider fixed power discrete rate method. Given fixed transmitter power per symbol E_s (or average SNR level $\bar{\gamma}=E_s/N_0$) and a target bit error rate (BER_{tg}), we adjust the modulation level M according to the instantaneous predicted channel gain in (10). Assume $\hat{\alpha}$ is the predicted channel gain at carrier f^1 and α is the actual gain at frequency f^2. The BER bound, i.e. $BER_{M(i)}^*(\bar{\gamma},\hat{\alpha})$, can be obtained as [8]:

$$BER_{M(i)}^*(\bar{\gamma},\hat{\alpha}) = \int_0^\infty BER_{M(i)}(\bar{\gamma}x^2)p_{\alpha|\hat{\alpha}}(x)\,dx \tag{13}$$

where $p_{\alpha|\hat{\alpha}}(x)$ is described by (9) and $BER_{M(i)}$ is calculated from the BER bound of MQAM for the AWGN channel [1]:

$$BER_{M(i)}(\gamma) \le 0.2exp(-1.5\gamma/(M(i)-1)) \qquad M(i)\ge 4 \tag{14}$$
$$BER_{M(1)}(\gamma) = Q(\sqrt{2\gamma}),$$

where γ is the instantaneous signal-to-noise ratio per symbol. (In a related technique in [4], noiseless outdated CSI is assumed available at the transmitter, and the expected bit error rate is calculated based on a conditional Rician distribution of the current channel amplitude.)

The thresholds α_i, $i=1\ldots4$ are chosen as follows. When the predicted channel gain $\hat{\alpha}$ satisfies: $\alpha_{i+1}\ge\hat{\alpha}\ge\alpha_i$, M(i)–QAM is employed, where $M(1)=2$, $M(i)=2^{2(i-1)}$, $i=2\ldots4$, ($\alpha_5=\infty$). The threshold α_i is the $\hat{\alpha}$ in (13) for which the bound $BER_{M(i)}^*(\bar{\gamma},\alpha_i) = BER_{tg}$. The average BER of this fixed power discrete rate adaptive modulation is lower than the BER_{tg} since the upper bound (14) is used and $BER_{M(i)}^*(\bar{\gamma},\hat{\alpha}) < BER_{tg}$ when $\hat{\alpha}$ does not take on a threshold value. Hence we utilize a power control policy to reduce the power consumption while maintaining the target BER. Once the modulation level M is decided for a particular $\hat{\alpha}$, a SNR level $\hat{\gamma}$ can be found by numerical search to maintain the target BER from (13). Note that $\hat{\gamma}$ is less than or equal to $\bar{\gamma}$. A similar power control method was proposed in [4].

The average bit per symbol (BPS) $\hat{R}_{ada}$ for both fixed and variable power methods is:

$$\hat{R}_{ada} = \sum_{i=1}^{4}\log_2 M_i \int_{\alpha_i}^{\alpha_{i+1}} p_{\hat{\alpha}}(x)dx, \tag{15}$$

where the pdf of predicted amplitude $p_{\hat{\alpha}}(x)$ is given by (8). This rate also gives the spectral efficiency assuming the ideal Nyquist data pulse. For the power control method above, the average signal to noise ratio γ_{avg} is

$$\gamma_{avg} = \int_0^\infty \hat{\gamma}(x)p_{\hat{\alpha}}(x)dx. \tag{16}$$

We plot the BPS (15) vs. the correlation coefficient ρ in (9) for different SNR computed from (16) with $BER_{tg}=10^{-3}$ in Fig.4. The correlation $\rho=1$ corresponds to perfect prediction, while $\rho=0$ represents the worst case when the BPS of the adaptive modulation converges to that of the non-adaptive M–QAM for given SNR and BER_{tg}.

The power control method above involves continuously varying transmitter power. It is possible to simplify it by associating each modulation level with constant transmitter power. This method is called discrete rate discrete power and was introduced for adaptive modulation with perfect CSI in [1]. For perfect CSI, the continuous power control policy achieves about 3dB gain relative to the fixed power discrete rate adaptive modulation, and the discrete rate discrete power method has power loss of less than 2dB relative to the continuous power discrete rate transmission scheme (see also [1]).

IV. Simulation Results and Performance Analysis

We use the Jakes model and our physical model to validate the performance of the continuous power discrete rate adaptive M–QAM aided by the LRP. The maximum Doppler shift of 100 Hz is used in both models. The target $BER=10^{-3}$. The fading signal is sampled at the rate of 500Hz for the LRP. The observation interval is 100 samples, the SNR in the observations is 80dB, the symbol rate is 25ksymbol/s, and the modulation-switching rate is the same as the symbol rate. Interpolation is utilized to predict the channel coefficients at the symbol rate. The prediction range is 2ms. The physical model in [9,12] is extended to include multiple frequencies [17]. The scenario for the physical model is shown in Fig.5. The reflectors are arranged to provide an approximately

exponential distribution of excess delay with the *rms* delay spread $\sigma \approx 1\mu s$.

In Fig. 6 we plot BPS vs. normalized frequency separation $\Delta f\sigma$ for the ideal (non-adaptive) MMSE filter (4-5) and the robust method using the LMS algorithm (10-11) with the step size 0.005. The parameters in (9) are estimated during the observation interval for both data sets and are used throughout the transmission. For example, for $\Delta f = 0$, the estimated $\rho = 0.983$ for the Jakes model and $\rho = 0.965$ for the physical model. The bit rate loss is less than half a bit for non-stationary data generated by the physical model relative to the stationary case. We also investigated the BPS under the assumption that prediction is perfect at frequency f^1. We observe that the performance of the robust algorithm is very close to this ideal case as well as to the performance of the ideal MMSE algorithm. This is consistent with the results in [8] where it is shown that when observations and the predicted samples are at the same frequency, performance of adaptive modulation aided by robust (adaptive) LRP closely approximates the ideal performance with perfect CSI. Hence the robust method is near-optimal and has the ability to adapt transmission parameters to the time-variant channel conditions. Moreover, for given σ, the theoretical value of the parameter ρ in (12) can be utilized in the selection of thresholds when robust prediction is used.

The performance of the adaptive modulation using the outdated CSI for the Rayleigh fading channel with the correlation function (3) is also shown in Fig.6. To alleviate the mismatch of the delayed and future CSI, a novel approach to calculate thresholds based on the delayed CSI was studied in [4]. A similar method is employed here. A single observation $c(f^1,n-1)$ is used instead of the estimate $\hat{c}(f^1,n)$ in (10) to compute the modulation parameters at frequency f^2. We found that even very small delay causes significant loss of the bit rate for fast vehicle speeds when accurate long range prediction is not utilized. For example, for $\Delta f\sigma=0$ and $\tau = 2$ms, the loss is 1 to 2 BPS. Thus, accurate LRP is required to achieve the bit rate gain of adaptive modulation for fast vehicle speeds and realistic delays.

Fig.6 also shows that adaptive modulation is primarily beneficial when the normalized frequency separation $\Delta f\sigma$ does not significantly exceed 0.1. For example, for $\Delta f\sigma = 0.1$, about 17dB is required to obtain 1 BPS for adaptive M-QAM as opposed to 24dB for non-adaptive signaling (BPSK). As $\Delta f\sigma$ approaches 0.4, the bit rate of adaptive modulation approximates that of non-adaptive transmission. Hence the frequency separation and the multipath delay (or the coherence bandwidth) are the factors that determine the performance of the proposed adaptive modulation method. The typical values of σ are on the order of microseconds in outdoor mobile radio channel [11]. Suppose $\Delta f\sigma = 0.1$ and $\sigma = 1\mu$ sec. Then the frequency separation $\Delta f = 100$KHz. This means that two channels can be separated by 100KHz and still benefit from the proposed adaptive transmission method.

Another practical consideration is the adaptation of the parameter ρ in (9) at the transmitter as a function of the variation of the *rms* delay spread σ. To investigate the limits on the speed of adaptation, we use the physical model to generate challenging and typical scenarios. In Fig.7, the variation of the *rms* delay spread is shown for three cases. For each scenario, the reflectors are arranged to give an approximately exponential excess delay distribution. The *rms* delay spread σ is slowly varying for case 1, a typical case. In the challenging cases 2 and 3, σ varies rapidly due to shadowing of many reflectors by a nearby structure during a portion of the track. We investigate the performance of adaptive modulation on these channels during the T=1 sec interval when σ varies rapidly in cases 2 and 3 (from 3.5 to 4.5 sec in Fig. 7). The variation of the *rms* delay spread is approximately from 0.7 to 2.3 μs and 0.4 to 2.6 μs for cases 2 and 3, respectively. The target BER is 10^{-3} and the power is adjusted to maintain the target BER to compensate for the mismatch of the *rms* delay. The parameter ρ is updated at the rate R_ρ Hz. Fig. 8 shows the BPS vs. SNR for the normalized adaptation rate $R_\rho T = 1$, i.e. the value of ρ is not updated during the interval T. There is about 2dB loss for the challenging case 3 relative to the *rms*-invariant case 1. To improve performance, the correlation ρ needs to be tracked and updated more frequently. Fig. 9 illustrates that there is significant performance loss for the challenging case if $R_\rho T < 2$. By analyzing datasets produced by the physical model, we concluded that the variation of the *rms* delay (and ρ) is typically slow and tracking of the correlation ρ does not result in significant additional computational and feedback load. The required rate of update of the parameter ρ is significantly slower than the low sampling rate for predicting at frequency f^1 in (10). Thus, the proposed robust prediction method based on the observations at a different carrier is feasible, but infrequent update of the time-variant frequency correlation is required to satisfy the adaptive transmission performance criterion (e.g. the BER_{tg}).

In this paper, the assumption of the exponentially distributed propagation delay (2) results in the relationship of the parameter ρ and the *rms* delay spread σ that is approximated by (12). If the distribution of the propagation delay is different, this relationship will change. For example, for the uniform distribution, the coherence bandwidth and ρ are reduced for a given σ, and hence the performance of the prediction in the frequency domain and the bit rate are degraded relative to the exponentially distributed excess delay. Since we directly estimate the correlation ρ from the dataset, our algorithm is robust to the variation in the distribution of the excess delay.

V. Conclusion

A novel adaptive modulation method that uses predicted CSI of a different carrier was presented. The statistical model of the prediction accuracy distribution was created, and system performance was evaluated for various frequency separation values and *rms* delay spreads. We demonstrated that

significant bit rate gains can be achieved relative to non-adaptive systems for realistic channel parameters, and that increased frequency separation and multipath delay limit the performance of adaptive transmission. We also used a novel physical model to investigate the rate of adaptation to the variation of the *rms* delay spread. The results in this paper give valuable insights into designing adaptive transmission methods for correlated carriers and multicarrier systems.

REFERENCES

[1] A.J. Goldsmith and S.G. Chua, "Variable-Rate Variable-Power MQAM for Fading Channels," *IEEE Trans. Comm*, vol. 45, No 10, Oct 1997, pp. 1218-1230.

[2] A. J. Goldsmith and S. G. Chua, "Adaptive Coded Modulation for Fading Channels," *IEEE Trans. Commun.*, Vol. 46, No. 5, May 1998, pp. 595 - 601.

[3] T. Ue, S. Sampei, N. Morinaga and K. Hamaguchi, "Symbol Rate and Modulation Level-Controlled Adaptive Modulation/TDMA/TDD System for High-Bit-Rate Wireless Data Transmission," *IEEE Trans. Veh. Technol.*, Vol. 47, No. 4, Nov. 1998, pp. 1134 - 1147.

[4] D.L. Goeckel, "Adaptive Coding for Time-Varying Channels Using Outdated Channel Estimates," *IEEE Trans. Commun*., Vol. 47, No. 6, June 1999, pp. 845-855.

[5] K. Miya, O. Kato, K. Homma, T. Kitade, M. Hayashi, and T. Ue, "Wideband CDMA Systems in TDD-mode Operation for IMT-2000," *IEICE Trans. Commun.,* Vol. E81-B, July 1998, pp.1317-1326.R.

[6] T. Eyceoz, A. Duel-Hallen, H. Hallen, "Deterministic Channel Modeling and Long Range Prediction of Fast Fading Mobile Radio Channels," *IEEE Commun. Lett.,* Vol. 2, No. 9, Sept. 1998, pp. 254 – 256.

[7] T. Eyceoz, S. Hu, and A. Duel-Hallen, "Performance Analysis of Long Range Prediction for Fast Fading Channels," *Proc. of 33rd Annual Conf. on Inform. Sciences and Systems CISS'99*, March 1999, Vol. II, pp. 656 - 661.

[8] S. Hu, A. Duel-Hallen, H. Hallen, "Long Range Prediction Makes Adaptive Modulation Feasible for Realistic Mobile Radio Channels," *Proc. of 34rd Annual Conf. on Inform. Sciences and Systems CISS'2000*, Vol. I, pp. WP4-7 ~ WP4-13, March 2000.

[9] A. Duel-Hallen, S. Hu and H. Hallen, "Long Range Prediction of Fading Signals: Enabling Adaptive Transmission for Mobile Radio Channels," *IEEE Signal Processing Mag.*, Vol. 17, No. 3, pp. 62 – 75, May 2000.

[10] W. C. Jakes, *Microwave Mobile Communications*. Wiley, New York, 1974.

[11] S. Rappaport, *Wireless Communications: Principles and Practice*. Prentice-Hall, 1996.

[12] H. Hallen, S. Hu, M. Lei and A. Duel-Hallen, "A Physical Model for Wireless Channels to Understand and Test Long Range Prediction of Flat Fading," *Proc. of WIRELESS 2001*, Calgary, Canada, July 9-11, 2001.

[13] J. G. Proakis, *Digital Communications*. Third Edition, McGraw-Hill, 1995.

[14] T. S. Yang, A. Duel-Hallen, "Adaptive Modulation Using Outdated Samples of Another Fading Channel," *Proc. IEEE Wireless Communications and Networking Conference,* vol. 1, pp. 477-481, Mar. 17-21, 2002.

[15] T. S. Yang, Ph.D. Thesis, NC State University, in preparation.

[16] J. Salz, "Optimum Mean-Square Decision Feedback Equalization," *Bell Syst. Tech. J*., Vol. 52, pp. 1341-1373,October, 1973.

[17] H. Hallen, A. Duel-Hallen, S. Hu, T. S. Yang, M. Lei, "A Physical Model for Wireless Channels to Provide Insights for Long Range Prediction," *Proc. MILCOM'02*, vol. 1, pp.627-631, Oct. 7-10, 2002.

[18] T. S. Yang, A. Duel-Hallen, H. Hallen, "Long Range Fading Prediction to Enable Adaptive Transmission at Another Carrier," *Proc. IEEE SPAWC'03,* June 15-18, 2003.

Tung-Sheng Yang received B.E. degree from the National Tsing Hua University, Taiwan in 1998 and M.S. degree from North Carolina University, NC 2000, both in Electrical Engineering. He is currently working toward the Ph.D degree in Electrical Engineering at the North Carolina University, NC.

His research interests include transmitter and receiver design for fading mobile radio channels, estimation and prediction of fading channels, and adaptive transmission for wireless mobile systems.

Alexandra Duel-Hallen received B.S. degree in mathematics from Case Western Reserve University in 1982, M.S. degree in Computer, Information and Control Engineering from the University of Michigan in 1983, and Ph.D. in Electrical Engineering from Cornell University in 1987. During 1987-1990

She was a Visiting Assistant Professor at the School of Electrical Engineering, Cornell University, Ithaca, NY. In 1990-1992, she was with the Mathematical Sciences Research Center, AT&T Bell Laboratories, Murray Hill, NJ. She is an Associate Professor at the Department of Electrical and Computer Engineering at North Carolina State University, Raleigh, NC, which she joined in January 1993.

From 1990 to1996, Dr. Duel-Hallen was Editor for Communication Theory for the IEEE Transactions on Communications. During 2000-2002, she has served as Guest Editor of two Special Issues on Multiuser Detection for the IEEE Journal on Selected Areas in Communications. Dr. Duel-Hallen's current research interests are in wireless and multiuser communications. Her 1993 paper was selected for the *IEEE Communications Society 50th Anniversary Journal Collection* as one of 41 key papers in physical and link layer areas, 1952-2002.

Hans Hallen received his B.S. degree in Engineering Physics from Cornell University in 1984, and his M.S. and Ph.D. degrees in applied physics from Cornell University in 1986 and 1991, respectively.

During 1991-1993, he was with the Physical Research Laboratory, AT&T Bell Laboratories, Murray Hill, NJ. He joined the North Carolina State University Physics Department in 1993, and is currently an Associate Professor. He has active projects in scanning proximal probe microscopy and spectroscopy, biophysics, lidar, and wireless communications.

List of figure captions

Fig. 1. Cross-correlation vs. normalized frequency separation $\Delta f\sigma$ for $\tau = 0$.

Fig. 2. System model.

Fig. 3. MMSE vs. normalized frequency separation $\Delta f\sigma$ for $f_s = 5\ f_{dm}$. Prediction range = $0.2/f_{dm}$.

Fig. 4. Bit per symbol vs. ρ for different SNR for power control M-QAM. Target BER=10^{-3}.

Fig. 5. *rms* delay spread for physical model.

Fig. 6. BPS vs. normalized frequency separation for different prediction techniques. $f_{dm} = 100$Hz. Prediction range is 2ms.

Fig. 7. The variation of the *rms* delay spread σ for typical (case 1) and challenging cases (cases 2 and 3).

Fig. 8. BPS vs. SNR for $R_\rho T = 1$. $\Delta f = 50$KHz.

Fig. 9. BPS vs. normalized adaptation rate $R_\rho T$. SNR = 20dB. $BER_{tg}=10^{-3}$. $\Delta f = 50$KHz.

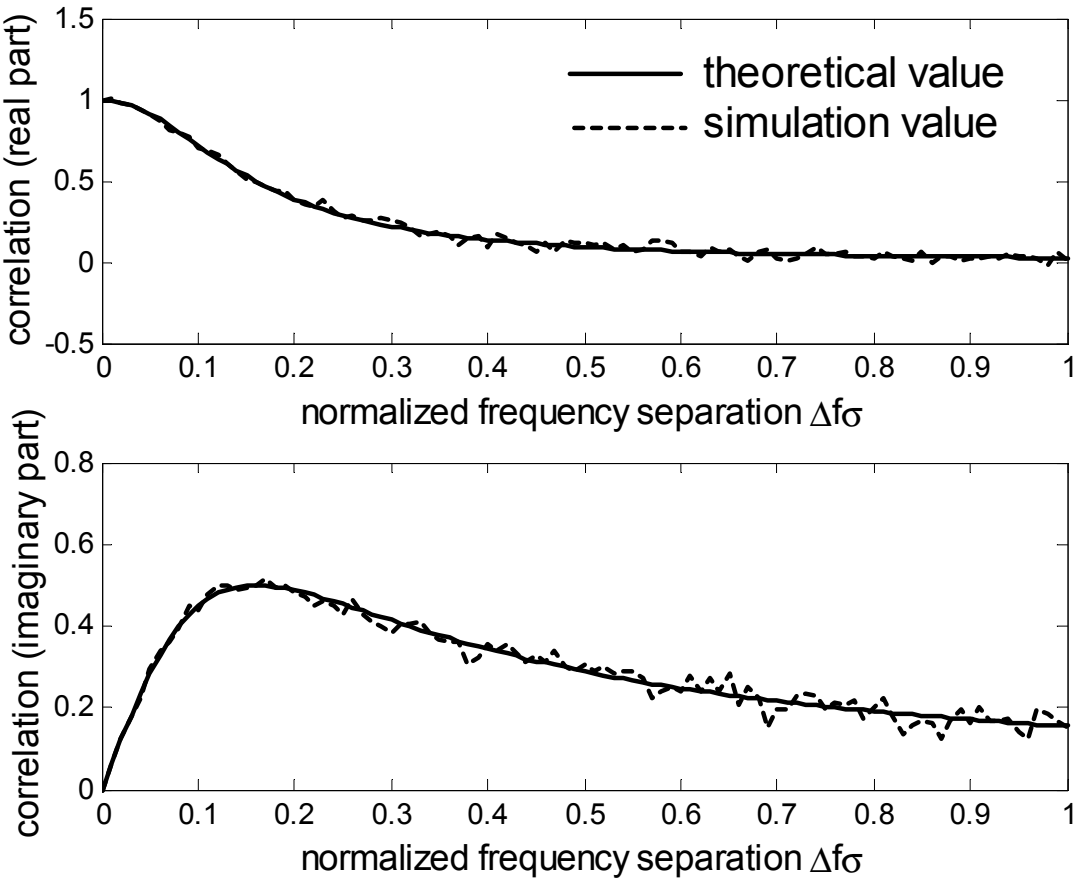

Fig. 1. Cross-correlation vs. normalized frequency separation $\Delta f\sigma$ for $\tau=0$.

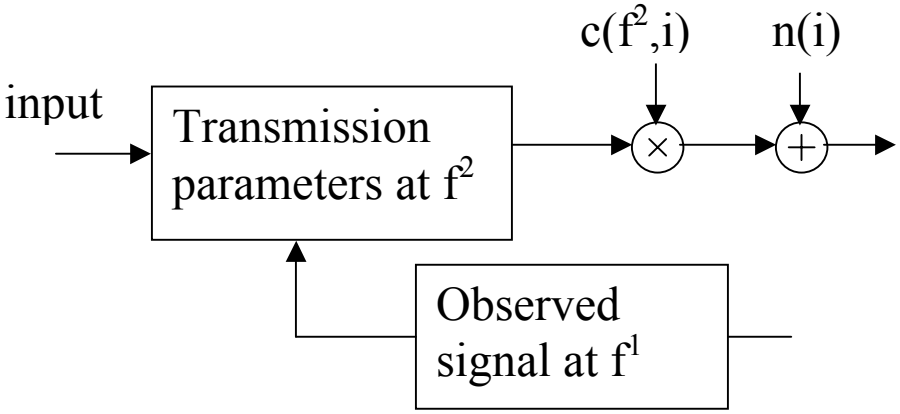

Fig. 2. System model.

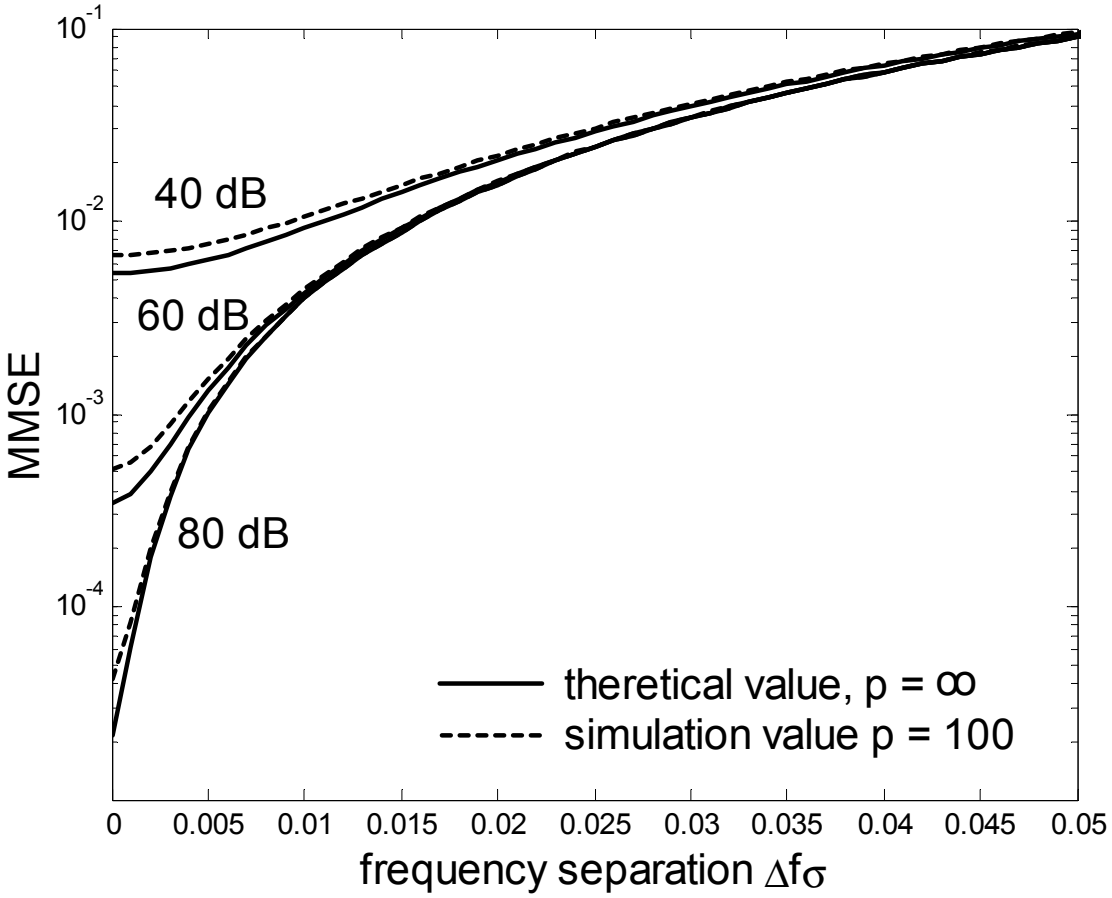

Fig. 3. MMSE vs. normalized frequency separation $\Delta f\sigma$ for $f_s = 5\ f_{dm}$. Prediction range $= 0.2/f_{dm}$.

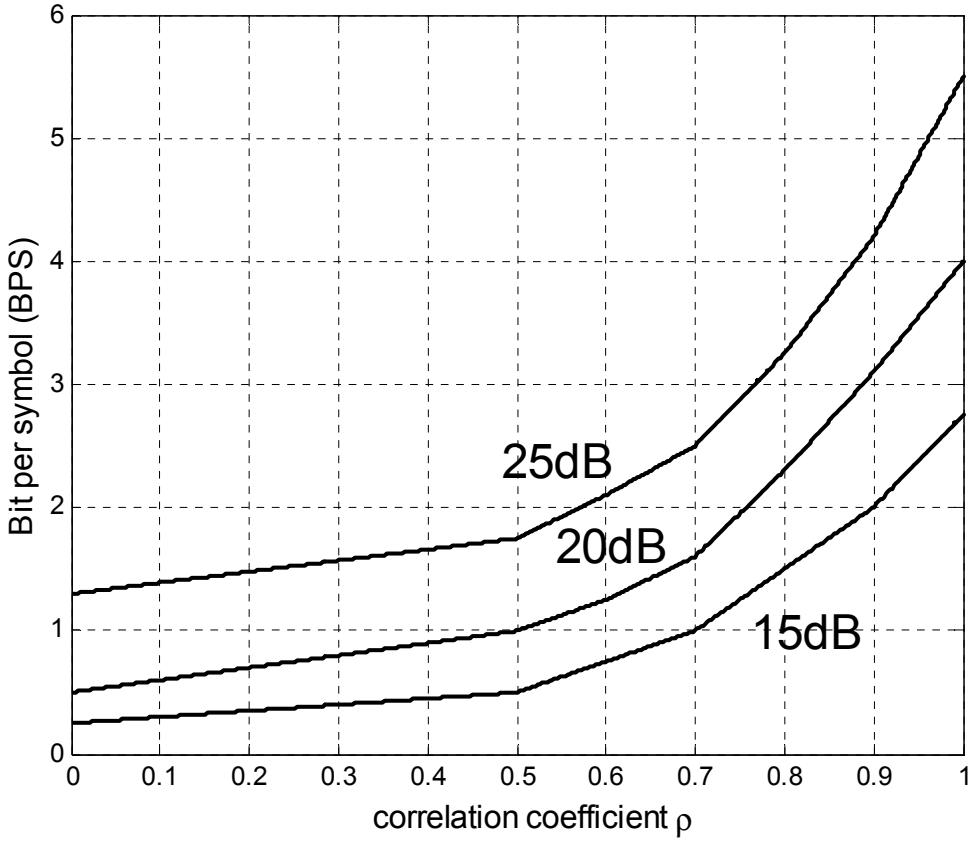

Fig. 4. Bit per symbol vs. ρ for different SNR for power control M-QAM. Target BER=10^{-3}.

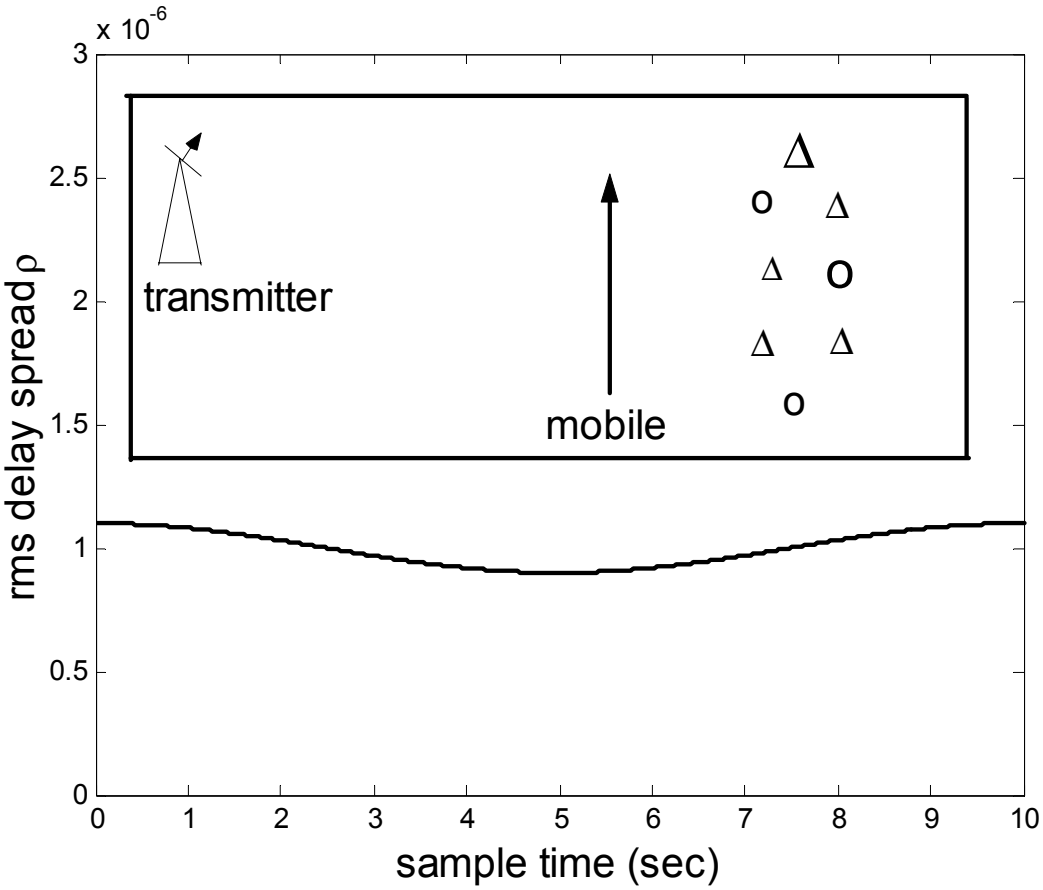

Fig. 5. *rms* delay spread for physical model.

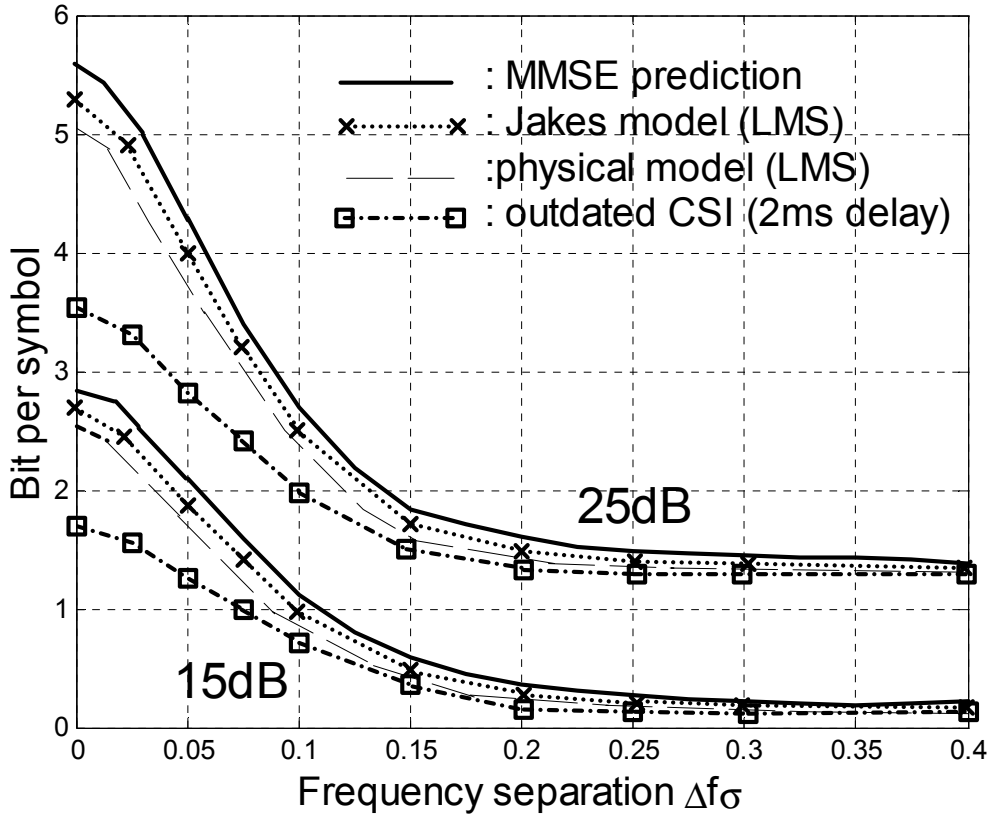

Fig. 6. BPS vs. normalized frequency separation for different prediction techniques. f_{dm} = 100Hz. Prediction range is 2ms.

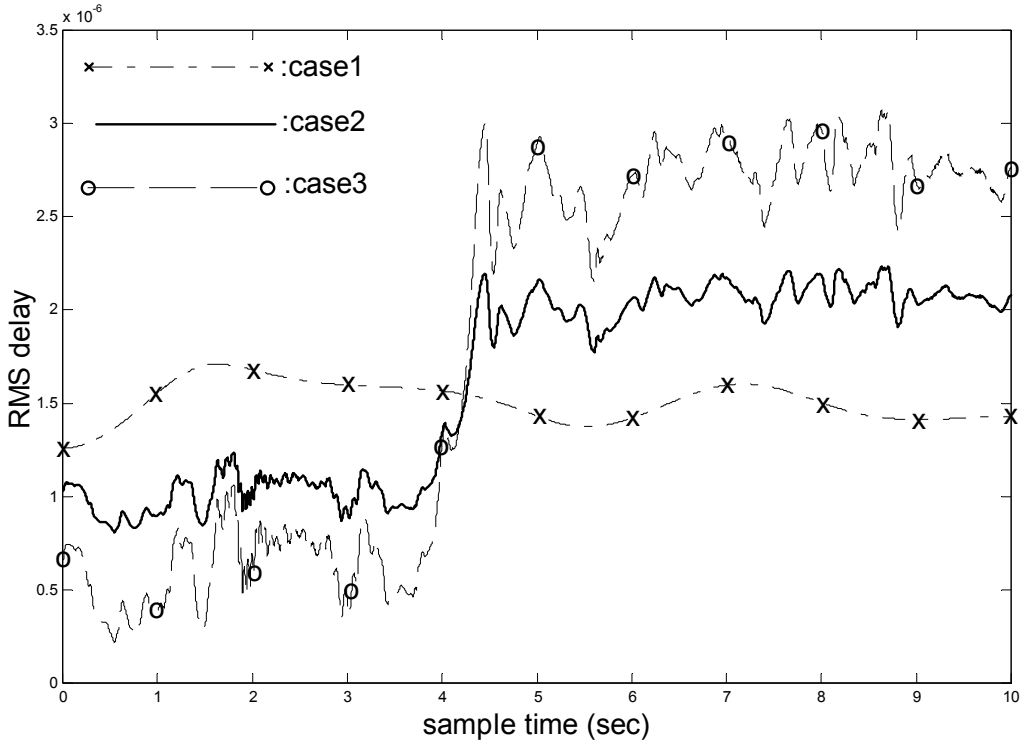

Fig. 7. The variation of the *rms* delay spread σ for typical (case 1) and challenging cases (cases 2 and 3).

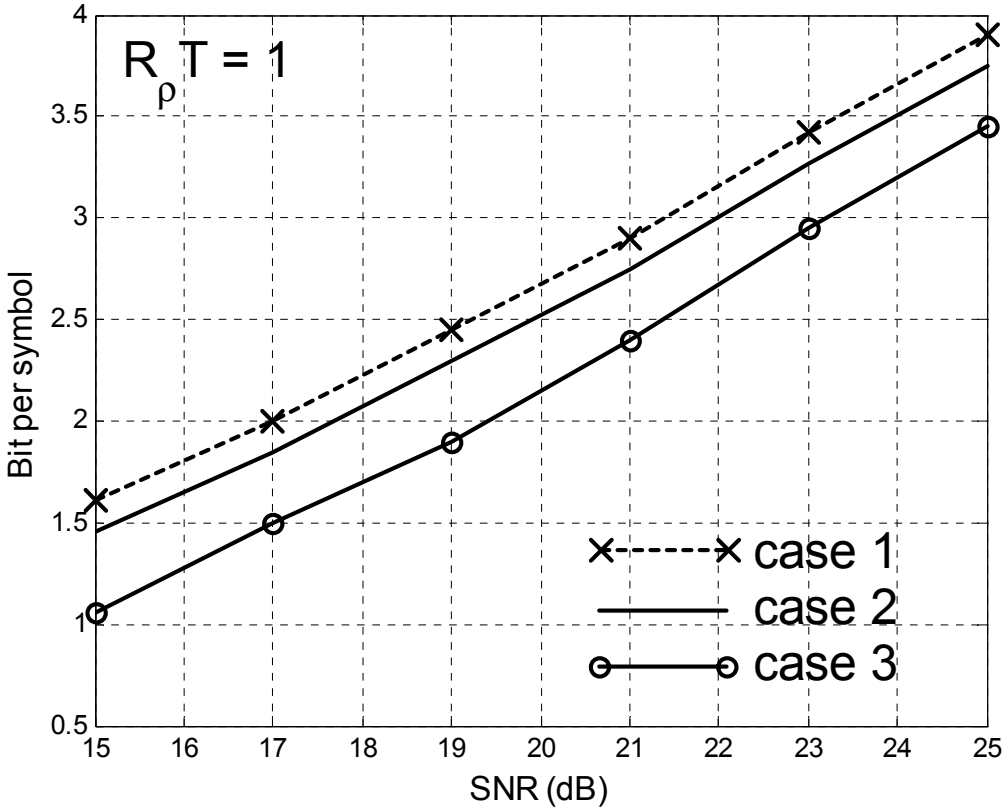

Fig. 8. BPS vs. SNR for $R_\rho T$ =1. Δf = 50KHz.

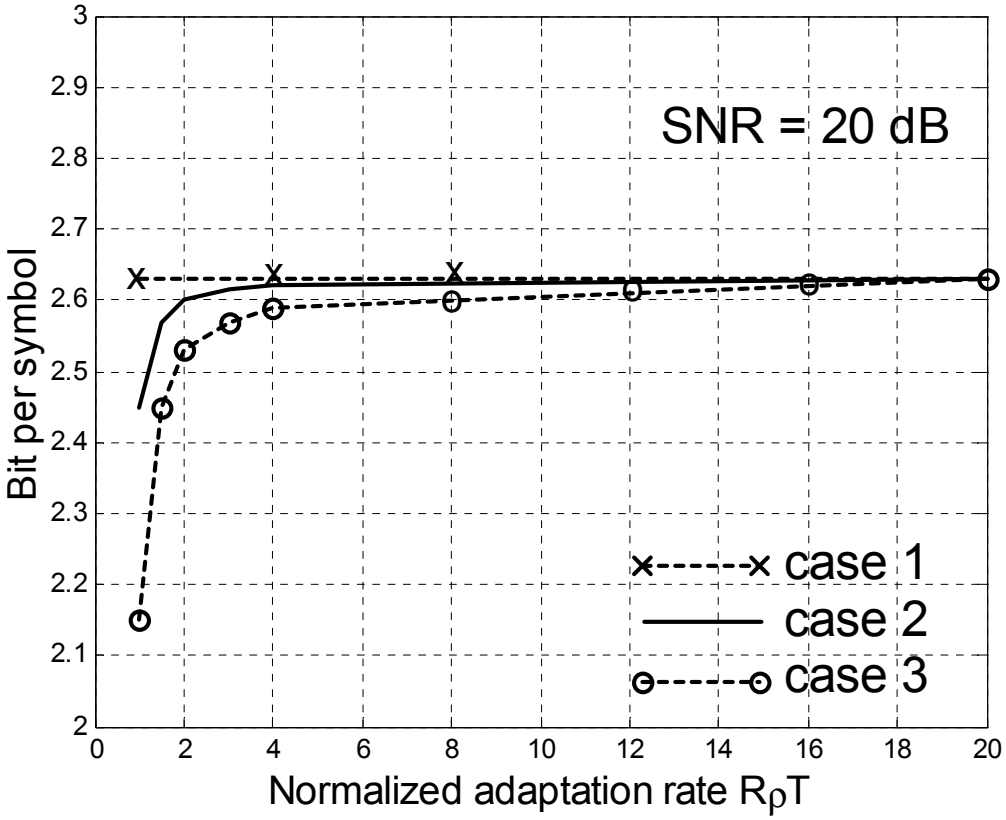

Fig. 9. BPS vs. normalized adaptation rate $R_\rho T$. SNR = 20dB. $BER_{tg}=10^{-3}$. Δf = 50KHz.